Tellus (1998), 50A, 1–11
Printed in UK – all rights reserved

Copyright © Munksgaard, 1998
TELLUS
ISSN 0280–6495

# Long-wave optical properties of water clouds and rain

By HANNU SAVIJÄRVI* and PETRI RÄISÄNEN, *Department of Meteorology, PO Box 4, 00014 University of Helsinki, Finland*

(Manuscript received 26 February 1997, in final form 23 June 1997)

ABSTRACT

Mie theory is used for calculation of the long-wave (5–200 μm) optical properties of non-precipitating and precipitating water clouds, and of rain. The optical parameters (mass extinction and absorption coefficients, coalbedo and asymmetry parameter) are then parameterized as simple functions of cloud drop effective radius, cloud water amount and rain rate, for use in general circulation and weather forecast models. Broadband and some wideband parameterizations are given and tested both in two-stream and emissivity applications. A simple relation between the effective radius and cloud water content is also suggested for maritime and continental air masses.

## 1. Introduction

The short-wave (SW) optical properties of clouds have been and are being very actively studied. The long-wave (LW) optical properties of water clouds have been less investigated lately. Instead, interest has been directed towards ice clouds in observations (Francis et al., 1994), in theoretical calculations, and in parameterizations for GCMs (Ebert and Curry, 1992). The reason may have been that GCM-produced water clouds tend to be fairly thick, making (model) clouds blackbodies; and that it has been thought that the strong water vapor absorption at water cloud altitudes renders the non-black cloud LW optics irrelevant, except perhaps in the window region (8–12.5 μm). However, the new generation GCMs and weather forecast models may be able to produce realistic tenuous clouds. Furthermore, the recent increase in the sophistication, resolution and accuracy of the clear-sky radiation schemes implies that increased attention should also be paid to the LW cloud optics.

Although high- and medium-resolution spectral Mie calculations for water cloud optics have been made in the long-wave region (Chylek and Ramaswamy, 1982; Chylek et al., 1992; Hu and Stamnes, 1993), these have been somewhat impractical for use in GCMs. Thus, the typical water cloud LW parameterization has been the use of a constant cloud mass absorption coefficient, often based on effective emissivity calculations (Stephens, 1978). However, the effective cloud emissivity by definition includes gas absorption, which then might be included twice in cloud layers unless care is taken to avoid this. Moreover, spectrally constant mass absorption may severely distort radiative transfer through a cloud layer, as the upward and downward fluxes entering a layer may be quite different spectrally (Stephens, 1984). Furthermore, the effect of drop size has been excluded in most LW schemes and the impact of rain has not been charted at all.

In this paper, Mie theory is used to derive the long-wave optical properties of various precipitating and nonprecipitating cloud drop distributions, and of rain. The calculations are extensions of the shortwave work by Savijärvi et al. (1997; SAR in what follows) to the long-wave region. Broad- and wide-band parameterization schemes are sug-

* Corresponding author.

gested, both for two-stream type applications, and for non-scattering applications (i.e., emissivity schemes), as functions of cloud effective radius $r_e$, cloud liquid water content LWC, and rain rate R. A simple parameterization for $r_e$ as a function of LWC, separating continental and maritime air masses, is also suggested.

## 2. The LW optics

The basic cloud optical properties needed for radiative transfer calculations are the nondimensional cloud optical depth $\tau(\lambda)$, single scattering albedo $\omega(\lambda)$ and asymmetry parameter $g(\lambda)$, $\lambda$ being wavelength. These are direct input into two-stream type LW radiation schemes (used in some GCMs), which allow scattering processes also in the longwave. If cloud- and raindrops are taken as steady water spheres in air (a good assumption except for the largest raindrops, which are flat and oscillate), these optical properties are given exactly by Mie theory. The volume extinction and absorption coefficients for a homogeneous drop ensemble (=cloud/rain layer) are in this case

$$\beta_{ext}(\lambda)=\int\pi r^2 Q_{ext}(x,c(\lambda))n(r)\mathrm{d}r\,, \tag{1}$$

$$\beta_{abs}(\lambda)=\int\pi r^2 Q_{abs}(x,c(\lambda))n(r)\mathrm{d}r\,, \tag{2}$$

where $r$ is the drop radius, $x=2\pi r/\lambda$ the Mie size parameter and $n(r)$ the dropsize distribution. $Q_{ext}$ and $Q_{abs}$ are the extinction and absorption efficiencies given by Mie theory. They are here calculated by the method of Bohren and Huffmann (1983), which has been slightly improved to allow better accuracy in the asymptotic case of very large (rain)drops. The complex refraction index of water $c(\lambda)$ is taken from Hale and Querry (1973). Integrals over $r$ are calculated numerically using $\Delta r=0.5$ µm in the cloud drop regime $r=$ 0.5–50 µm and $\Delta r=50$ µm in the rain drop regime $r=50$–2000 µm.

The optical depth of a vertically homogeneous (cloud) layer is $\tau(\lambda)=\beta_{ext}\Delta z$. It is a measure of transmission through the layer. The single scattering coalbedo, which is a measure of absorption, is $1\text{-}\omega(\lambda)=\beta_{abs}/\beta_{ext}$. The asymmetry factor $g(\lambda)$ of a cloud layer, a measure of how strongly scattering is concentrated into the forward direction, is calculated here as given in SAR.

Cloud drop absorption is fairly strong in the longwave ($1\text{-}\omega\approx 0.5$ as will be seen later). Furthermore, drop scattering is mostly in the forward direction ($g$ is close to 1 as will be seen later), and the radiation field is more isotropic in the longwave than in the shortwave regime so its redistribution by scattering is less important (Fouquart 1988). Therefore the so-called absorption or no-scattering approximation is common in the longwave regime. The cloud LW optics is then governed solely by the monochromatic cloud beam emissivity $\varepsilon_b$ (or beam transmissivity $t_b$):

$$\varepsilon_b(\lambda)=1-\exp(-\kappa_c(\lambda)\mathrm{LWP}),\qquad t_b(\lambda)=1-\varepsilon_b(\lambda)\,, \tag{3}$$

where LWP is the cloud layer (vertical) liquid water path; LWP$=$LWC$\Delta z$, LWC being the cloud liquid water content. The beam mass absorption coefficient $\kappa_c(\lambda)$ is

$$\kappa_c(\lambda)=\beta_{abs}(\lambda)/\mathrm{LWC}\,. \tag{4}$$

Eq. (3) can be used to estimate $\kappa_c$ from flight observations of beam radiances within clouds. These are usually made at the water vapor window wavelengths near 9 or 11 µm. In models, flux calculations are more relevant. The monochromatic flux emissivity $\varepsilon(\lambda)$ is given to a good accuracy (Liou 1992) by:

$$\varepsilon(\lambda)=1-\exp(-D\kappa_c(\lambda)\mathrm{LWP})\,, \tag{5}$$

where $D$ is the diffusivity factor. Quite often, $D$ is absorbed in the numerical value of $\kappa_c$. We, too, adopt this "flux" mass absorptivity convention with the value of $D=1.66$; thus $k_c=D\kappa_c$ in what follows.

In GCM schemes, averaging over wavelength is necessary for practical reasons. The wavelength averages are obtained by weighing with the Planck function $B_\lambda(T)$, so that for $s(\lambda)$ ($s=\beta_{ext}$, $1\text{-}\omega$, $g$, $k_c$, $\varepsilon$) the average over a band $\Delta\lambda$ is given by

$$s(T)=\int_{\Delta\lambda}s(\lambda)B_\lambda(T)\mathrm{d}\lambda\Big/\int_{\Delta\lambda}B_\lambda(T)\mathrm{d}\lambda\,, \tag{6}$$

broadband values being valid for $\Delta\lambda=5$–200 µm. In particular, the accuracy of the widely adopted "grey" approximation,

$$\varepsilon\approx 1-\exp(-k_c(T)\mathrm{LWP}))\,, \tag{7}$$

will be studied. The temperatures of $-10$°C and 20°C are used to demonstrate the dependence of the LW optics on cloud layer temperature.

## 3. Cloud and raindrop size distributions and some asymptotic results

The cloud and rain drop number concentration $N$, liquid water content LWC and the effective radius $r_e$ are integrals over the drop size distribution $n(r)$:

$$N=\int n(r)\mathrm{d}r, \qquad \mathrm{LWC}=(4\pi\rho/3)\int r^3 n(r)\mathrm{d}r,$$

$$r_e=\int r^3 n(r)\mathrm{d}r/\int r^2 n(r)\mathrm{d}r, \tag{8}$$

$\rho$ being the density of liquid water. 14 cloud drop size distributions (described in detail in SAR) are used in this study; they are mainly from Slingo and Schrecker (1982) (Fig. 1a) and from the LOWTRAN-7 radiation package (Fig. 1b). Fig. 2 shows, as in SAR, $r_e$ versus LWC calculated via (8) for these 14 drop distributions of nonprecipitating clouds. Linear regression gives $r_e=5+8$ LWC ($r_e$ in µm, LWC in g m$^{-3}$) as an overall relation between $r_e$ and LWC, using all points. This was suggested in SAR.

However, there seem to be two sets of points in Fig. 2. The upper set consists of clouds with large $r_e$ but low $N$ (25–280 drops/cm$^3$) for their LWC. These may be taken as "maritime" clouds, and for them, $r_{e,m}\approx 5.5+9.5$ LWC. The lower set consists of clouds with small $r_e$ but high $N$ (120–440 drops/cm$^3$). These are "continental" clouds, and for them, $r_{e,c}\approx 4.0+7.0$ LWC. The two relations produce a simple first approximation for $r_e$ if LWC is known while providing a division between continental and maritime clouds. The suggested "continental" relation gives values close to those used in the Canadian Climate Centre model, which gave good results in the observational validation of Johnson (1993) for continental clouds (but not for maritime clouds). The "maritime" relation can be validated, e.g., from the measured in-situ droplet properties through the marine stratocumulus in Nicholls (1984). The result is consistent with the $r_{e,m}$ above.

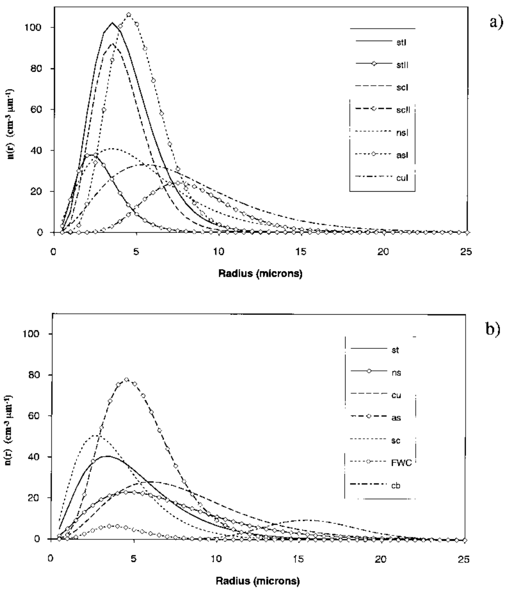


*Fig. 1.* The 14 droplet size distributions used. For further explanation, see Table 1 in Savijärvi et al. (1997). a) The SS82 set, b) The LOWTRAN-7 set.

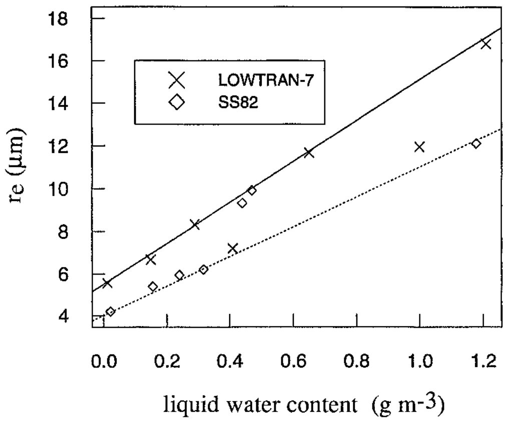


*Fig. 2.* The effective radius $r_e$ (µm) as a function of liquid water content (gm$^{-3}$) for the 14 cloud drop distributions shown in Fig. 1. The lines are the "maritime" and "continental" parameterizations suggested in the text.

We do not need these linear relations in this article but note that they have the advantage of producing finite $r_e$ for small LWC, as has been observed. The suggested $r_e\approx \mathrm{LWC}^{1/3}$ (Martin et al., 1994) and $r_e\approx \mathrm{LWP}^{1/6}$ (Pontikis and Hicks, 1992) relations tend to give unrealistically small $r_e$ for small LWC. The physical reason for finite $r_e$ is the fact that once the embryo drops become activated, they grow very fast by diffusion in conditions typical for clouds. Only in surface radiation fogs (with small supersaturation and numerous condensation nucleii) are values of $r_e$ sometimes observed to be less than about 4 µm.

Our rain drop size distributions are lognormal and are the same as those used in SAR. A precipitating cloud layer is the sum of cloud drop and rain drop size distributions. In SAR shortwave parameterizations were developed for such precipitating clouds. In Savijärvi (1997) the SW optics of rain were determined and parameterized directly. We follow this latter alternative here by parameterizing the cloud and rain LW optics separately. They can be combined for layers containing both cloud and rain; in the two-stream schemes by:

$$\tau=\tau_c+\tau_r\,,$$
$$\omega=(\tau_c\;\omega_c+\tau_r\omega_r)/\tau\,, \tag{9}$$
$$g=(\tau_c\omega_c g_c+\tau_r\omega_r g_r)/(\tau\omega)\,,$$

and in the absorptivity approximation by multiplying the transmissivities: $t=t_c t_r$. Subindexes $_c$ and $_r$ refer to the cloud-only and rain-only values. The gaseous transmissivities ($t_g$) or gas optics ($\tau_g$, $\omega_g=0$, $g_g=0$) can be included in an analogous fashion. For instance, the effective emissivity is $\varepsilon_{eff}=1-t_g t_c t_r$ if there is no strong correlation between the gas, cloud and rain absorption spectra.

Fig. 3 presents water drop $Q_{ext}$ and $Q_{abs}$ as a function of drop radius for wavelengths 9 and 11 μm. $Q_{ext}$ at $\lambda=9$ μm shows a typical Mie peak near $r=10$ μm while for $r>20$ μm, $Q_{ext}$ asymptotes exactly to 2 independent of wavelength, and $Q_{abs}$ roughly to 1. Use of $Q_{ext}=2$, $Q_{abs}\approx 1$ for all $r$ in (1)–(5) leads to the "large absorbing drop approximation". Then, at all wavelengths

$$\beta_{ext}/\mathrm{LWC}=\tau/\mathrm{LWP}=3/(2\rho r_e), \qquad \omega\approx 0.5,$$
$$k_c\approx 3D/(4\rho r_e)\,. \tag{10}$$

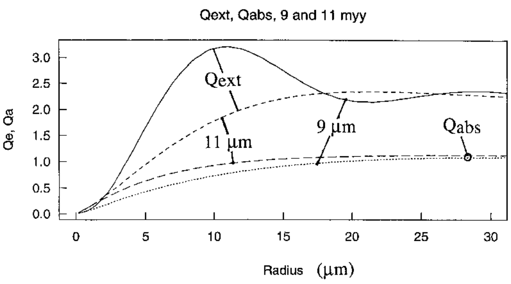


*Fig. 3.* The Mie extinction and absorption efficiences $Q_{ext}$ and $Q_{abs}$ at $\lambda=9$ and $\lambda=11$ μm for cloud drops as a function of drop radius $r$ (μm).

The relation $k_c\approx r_e^{-1}$ has been validated from observations in ice clouds, where all particles tend to be large (Francis et al., 1994).

On the other hand, $Q_{ext}$ and $Q_{abs}$ grow nearly linearly with $r$ for small $r$ in Fig. 3. Assuming constant growth rate leads to the "small absorbing drop approximation" (Chylek, 1978; Stephens, 1984). In this case $k_c$ and $\tau$/LWP are independent of $r_e$ at a fixed LW wavelength. This state of affairs has been verified for radiation fogs (Pinnick et al., 1979), which consist of small drops only. A typical water cloud contains both small and large drops, and will fall somewhere between these two asymptotic cases.

## 4. Results

### *4.1. Cloud LW optics as a function of wavelength*

Fig. 4 presents $\beta_{ext}$ (km$^{-1}$), 1-$\omega$ and $g$ as functions of $\lambda$ for a small-drop cloud (continental stratocumulus scI; $r_e=5.4$ μm), for a medium-dropsize cloud (maritime stratocumulus scII, $r_e=9.9$ μm), for a large-drop cloud (nonprecipitating cumulonimbus cb, $r_e=16.7$ μm), and for a precipitating cb with a rain rate of $R=50$ mm/h ($r_e=44$ μm). The non-precipitating cloud values are broadly similar to earlier calculations (Stephens, 1979). The volume extinction coefficient $\beta_{ext}$ shows a minimum at 11–12 μm for all clouds, and a clear maximum at 9–10 μm for the larger-drop clouds. Since both wavelengths are in the gaseous window region, this difference could perhaps be utilized in remote sensing for the detection of drop size. $\beta_{ext}$ is in general larger for large-drop clouds because of their larger water content. Raindrops have only a marginal effect on $\beta_{ext}$ in the precipitating cb.

The coalbedo 1-$\omega$ is mainly between 0.4 and 0.6 for the large-drop clouds. Precipitation has only a minor effect on 1-$\omega$. The small-drop nonprecipitating clouds show more variation with wavelength and $r_e$, displaying large values (1-$\omega\approx$ 0.6–0.8) beyond 12.5 μm, and small values (0.2–0.3) at 7–12.5 μm. For two-stream methods, 12.5 μm is thus a natural spectral band boundary.

The asymmetry factor $g$ is 0.85–0.90 at 5–12.5 μm, so cloud drops scatter strongly forward in this spectral region with only a modest dependence on $r_e$. At longer wavelengths, drops are small compared to $\lambda$ and scattering becomes less directional. Large rain drops are too few to make an

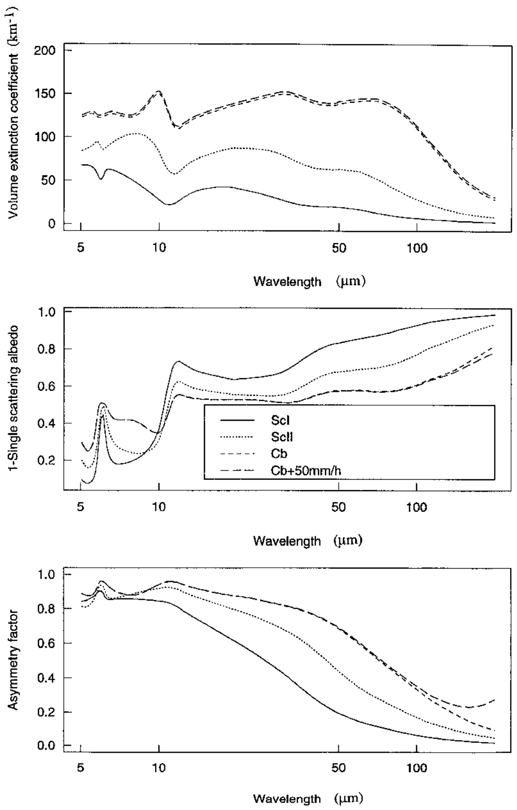


*Fig. 4.* The volume extinction coefficient $\beta_{ext}$ ($km^{-1}$), coalbedo 1-$\omega$, and asymmetry parameter $g$ as a function of wavelength $\lambda$ (μm) in the longwave region 5–200 μm, for scI, scII and cb clouds, and for cb with rain rate 50 mm/h. (Mie theory calculations).

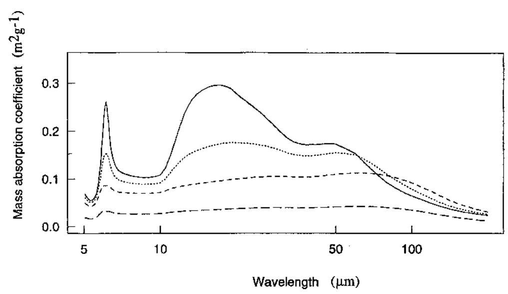


*Fig. 5.* As Fig. 4 but for the (flux) mass absorption coefficient $k_c(\lambda)$ ($m^2g^{-1}$).

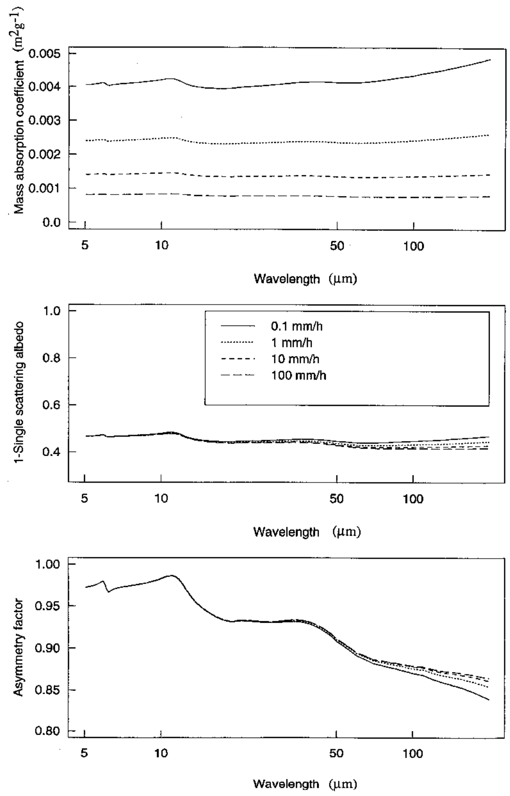


*Fig. 6.* The mass absorption coefficient $k_c$ ($m^2g^{-1}$), coalbedo 1-$\omega$ and asymmetry parameter $g$ as a function of wavelength $\lambda$ (μm) in the longwave region 5–200 μm, for rain with intensity 0.1, 1, 10 and 100 mm/h.

impact in the precipitating cloud (although $g_r > 0.85$ throughout the LW region, Fig. 6). Thus, in a precipitating cloud, $g$ is insensitive to the rain rate, as was 1-$\omega$.

Fig. 5 displays the "flux" mass absorption coefficient $k_c(\lambda)$. For small-drop clouds, the small absorbing drop approximation is nearly valid. Then, at each wavelength, $k_c$ is directly proportional to the strength of absorption, which is determined by the imaginary part of the refractive index $c_i(\lambda)$. Therefore, $k_c(\lambda)$ of the small-drop cloud (scI) in Fig. 5 is similar in shape to $c_i(\lambda)$, showing large variations along $\lambda$ with less absorption (a "droplet window") at 7–10 μm. For larger-drop clouds, the wider droplet spectrum and the inverse dependence of $k_c$ on $r_e$ for large drops reduce the values of $k_c$ and smooth out its variations along $\lambda$. For the precipitating cb, the mass absorption coefficient is less than half of that for the nonprecipitating cb.

Some observational estimates are available for $k_c$. They are based on vertical narrowband radiance measurements through low-level water clouds (mostly stratocumulus), and are listed in Stephens (1984). These radiance observations are from the water vapour window so the values are presumably not too much contaminated by gaseous absorption. The range for $k_c$ is $0.11–0.15\ \mathrm{m^2 g^{-1}}$ at 10–12 μm. This is in good agreement with the Mie-based $k_c$ values of scI and scII in Fig. 5 for the same spectral interval.

Although there is the droplet window in $k_c$ for small-drop clouds at 7–10 μm, it may be safe to say that correlation between the absorptivity spectrum of clouds (Fig. 5), and the absorptivity spectrum of the atmospheric gases (with their window at 8–12.5 μm) is not strong, at least not for large-drop clouds. Thus the effective emissivity -type broadband formulations ($t = t_{\mathrm{cloud}} t_{\mathrm{gas}}$; $\varepsilon_{\mathrm{overlap}} = 1$ — $(1\text{-}\varepsilon_{\mathrm{cloud}})(1\text{-}\varepsilon_{\mathrm{gas}})$, Stephens, 1984) are feasible.

### 4.2. *Rain LW optics and parameterizations*

Fig. 6 presents the mass absorption coefficient $k_c$, coalbedo 1-$\omega$ and asymmetry parameter $g$ as functions of $\lambda$ for the lognormal rain drop size distribution with intensities $R = 0.1$ mm/h (drizzle), 1 mm/h (weak), 10 mm/h (moderate) and 100 mm/h (heavy rain). The values of $k_c$ are small and are nearly constant with $\lambda$. They follow the large absorbing drop approximation (10) quite closely. Likewise, 1-$\omega$ is $\approx 0.5$ for all $\lambda$ and $R$ in Fig. 6, as expected for large absorbing particles. The asymmetry parameter $g$ is $>0.9$ for $5 < \lambda < 50$ μm. Thus LW scattering from raindrops is strongly forward-directed throughout the thermal region.

Utilizing the relations between the rainwater content, the effective radius $r_e$ and the rain rate $R$ in the lognormal rain drop size distribution, given in Savijärvi (1997), one gets the following parameterizations for the LW optics of rain as a function of $R$:

for two-stream methods: $\tau_r = 0.00018\ R^{0.67} \Delta z$,

$1 - \omega_r = 0.45, \quad g_r = 0.95$,

for emissivity schemes: $k_c = 0.0025\ R^{-0.23}$,

$\varepsilon_r = 1 - \exp(-0.00015 R^{0.67} \Delta z)$,

where $R$ is in mm/h, $k_c$ in $\mathrm{m^2\ g^{-1}}$, and $\Delta z$ is the height of the precipitation layer in m. These relations are independent of wavelength to the extent seen in Fig. 6. The optical depth $\tau_r$ in the LW region is the same as in the SW region. Thus the alternative SW formulations of Savijärvi (1997) are valid also in the longwave. One may finally note that a 1 km deep rain layer (e.g., in the PBL below a precipitating cloud) of moderate intensity ($R = 10$ mm/h) is semitransparent (it produces a LW emissivity of 0.50), while that of heavy rain ($R = 100$ mm/h) is close to a blackbody with $\varepsilon_r$ of 0.96.

### 4.3. *Parameterizations for nonprecipitating clouds*

Fig. 7a shows the broadband (5–200 μm) $k_c(T)$ values ($\mathrm{m^2 g^{-1}}$) of the 14 non-precipitating clouds as a function of $r_e$ (μm), for two cloud layer temperatures: $T = 20$°C and $-10$°C. The bulk mass absorption coefficient is clearly insensitive to ambient temperature but decreases with $r_e$. Shown in Fig. 7a is also the large-drop approximation (10; dotted line); the ECHAM4 formulation (Roeckner et al., 1996; long-dashed line), our simple parameterization (11) (solid line):

$$5\text{–}200\ \mu\mathrm{m}: \qquad k_c = 0.31\ \exp(-0.08\ r_e), \tag{11}$$

and the upflux and downflux coefficients used in the ECMWF model (the lower and upper short-dashed lines, respectively). The large-drop approximation is actually not bad except for the smallest-drop clouds. The ECHAM4 formulation, based on independent cloud drop size distributions and Mie calculations, is excellent. The very small variance of our results around it, and around (11), confirms for the LW region the conclusions of Hu and Stamnes (1993): details in the drop size distributions (variance, modality etc.) are not important, $r_e$ describing in solo the cloud microphysics for the atmospheric optics. Note specifically that the "marine" and "continental" clouds do not pop out in Fig. 7 as they did in Fig. 2.

However, the strong variation of $k_c$ along $\lambda$, in particular the "droplet window" at 7–10 μm seen in Fig. 5, implies that $k_c$ should really be spectral. A coarse but potentially very useful way is to define an average $k_c$ for the gaseous window band 8–12.5 μm; for the water vapour vibration-rotation band 5–8 μm; and for the far-infrared band 12.5–200 μm. The gaseous window is separ-

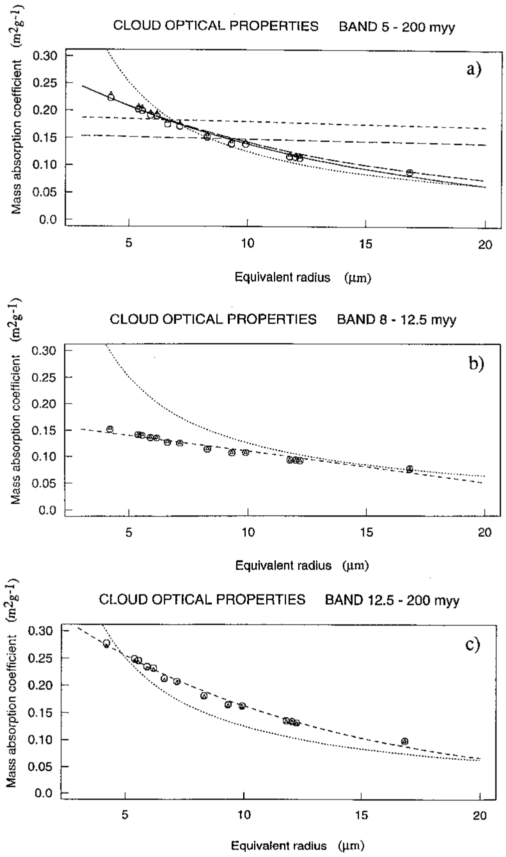


*Fig. 7.* (a) The broadband (5–200 µm) mass absorption coefficient $k_c(T)$ (m$^2$g$^{-1}$) for 14 non-precipitating clouds as a function of effective radius $r_e$ (µm), at $T=20$°C (circles) and $T=-10$°C (triangles). The curves are parameterizations described in the text. (b) As (a) but for the gaseous window region, 8–12.5 µm. The dashed line is eq. (12 b2). (c) As (a) but for the far-infrared region, 12.5–200 µm. The dashed line is eq. (12 b3).

ated out in most longwave radiation schemes, and spectral details in the non-window regions are less important because of the strong gaseous absorption there. Figs. 7b, c present our results for the 8–12.5 µm and 12.5–200 µm bands. The large-drop approximation is again quite valid for the largest-drop clouds independent of wavelength, as it should be. In the window region, $k_c$ is only weakly varying with $r_e$ and linear regression gives a good fit. In the far-infrared band the mass absorptivity is stronger and exponential decay is more appropriate. The dependence on temperature is not important. We thus suggest the following three-band cloud emissivity scheme:

$$\text{b1:} \quad 5\text{–}8\ \mu\text{m:} \quad k_c = 0.15\text{–}0.005\ r_e\,,$$

$$\text{b2:} \quad 8\text{–}12.5\ \mu\text{m:} \quad k_c = 0.17\text{–}0.006\ r_e\,, \tag{12}$$

$$\text{b3:} \quad 12.5\text{–}200\ \mu\text{m:} \quad k_c = 0.40\ \exp(-0.09\ r_e)\,.$$

These are shown as dashed lines in Figs. 7b, c. For the 8–12.5 µm window region, the $k_c$ values given by (12) are around 0.10–0.13 for medium-dropsize clouds. Stephens (1978) derived the average value of 0.116 for a 8.33–13.9 µm window from theoretical effective emissivity calculations. This value was in good agreement with narrowband observations in Stephens et al. (1978).

As the values of $k_c$ and their dependence on $r_e$ start to grow strongly at 10 µm (as seen in Fig. 5 and pointed out earlier, e.g., by Chylek and Ramaswamy, 1982), it could be beneficial to further divide the 8–12.5 µm region into 8–10 µm and 10–12.5 µm sub-bands. 10 µm is also a natural boundary in LW schemes because of the 9.6 µm ozone band. Thus a four-band cloud LW emissivity scheme might consist of the 5–8 µm and 12.5–200 µm band parameterizations as given in (12), and of the following:

$$\text{b2a:} \quad 8\text{–}10\ \mu\text{m:} \quad k_c = 0.12\text{–}0.003\ r_e\,, \tag{13}$$

$$\text{b2b:} \quad 10\text{–}12.5\ \mu\text{m} \quad k_c = 0.25\ \exp(-0.07\ r_e)\,.$$

A final question is how good the widely used "grey" approximation is. This is demonstrated in Table 1, where the exact $\varepsilon(\lambda)$ from (5) is averaged over 5–200 µm via (6), and compared to the use of the spectrally averaged $k_c(T)$ in (7). The calculation is for the LOWTRAN-7 stratocumulus drop distribution at $-10$°C but the conclusions are similar for other clouds and temperatures. The greybody approximation gives a slight overestimate for the cloud emissivity for all LWPs. However, the difference is quite small. For the important gaseous window region in (12), the difference is even smaller, as $k_c$ displays less spectral variation there. Thus the broadband approximation (11) would be quite good for clouds alone. However, the rapid gaseous variation makes things more complicated when clouds and gas absorption are combined, analogously to the situation in the near-infrared region of solar radiation.

Table 1. *The exact* $\varepsilon(\lambda)$ *of (5) averaged over 5–200 µm via (6), and the grey approximation (7) using spectrally averaged* $k_c(T)$

| LWP (g m$^{-2}$) | Exact ε | Grey ε | Grey-exact |
|---|---|---|---|
| 0.5 | 0.086 | 0.086 | 0.000 |
| 1 | 0.165 | 0.166 | 0.001 |
| 2 | 0.301 | 0.305 | 0.004 |
| 3 | 0.412 | 0.420 | 0.008 |
| 5 | 0.582 | 0.597 | 0.015 |
| 8 | 0.743 | 0.766 | 0.023 |
| 10 | 0.811 | 0.837 | 0.026 |
| 20 | 0.952 | 0.974 | 0.022 |

The calculation is for the LOWTRAN-7 stratocumulus drop distribution (250 drops/cm$^3$, $r_e = 6.64$ µm, LWC = 0.15 g m$^{-3}$) at cloud temperature of −10°C ($k_c(T) = 0.182$ m$^2$g$^{-1}$).

For the two-stream methods, Fig. 8 presents the broadband mass extinction coefficient $\beta_{ext}$/LWC, the coalbedo and the asymmetry parameter as functions of $r_e$ for the 14 clouds. Scatter among the cloud points is again small. The dependence on cloud temperature is slightly larger than in $k_c$ but small enough that it is disregarded in the following simple yet fairly accurate bulk parameterizations:

$$\begin{aligned} &\tau_c = \text{LWP}\ (0.29\text{–}0.012\ r_e), \\ \text{5–200 µm:}\quad &1-\omega_c = 0.54\text{–}0.0045\ r_e, \qquad (14) \\ &g_c = 1\text{–}0.36\ \exp(-0.07\ r_e), \end{aligned}$$

which are shown in Fig. 8 as solid lines. The three-band parameterizations are, respectively, (dropping the subindex c for brevity):

$$\begin{aligned} \text{b1:}\quad &\tau = \text{LWP}\ 0.70\ \exp(-0.12\ r_e), \\ &1-\omega = 0.11 + 0.018\ r_e, \\ &g = 0.84 + 0.003\ r_e, \\ \text{b2:}\quad &\tau = \text{LWP}\ (0.24\text{–}0.008\ r_e), \\ &1-\omega = 0.43\text{–}0.003\ r_e, \\ &g = 1\text{–}0.25\ \exp(-0.08\ r_e), \qquad (15) \\ \text{b3:}\quad &\tau = \text{LWP}\ (0.27\text{–}0.011\ r_e), \\ &1-\omega = 0.74\text{–}0.014\ r_e, \\ &g = 1\text{–}0.5\ \exp(-0.07\ r_e). \end{aligned}$$

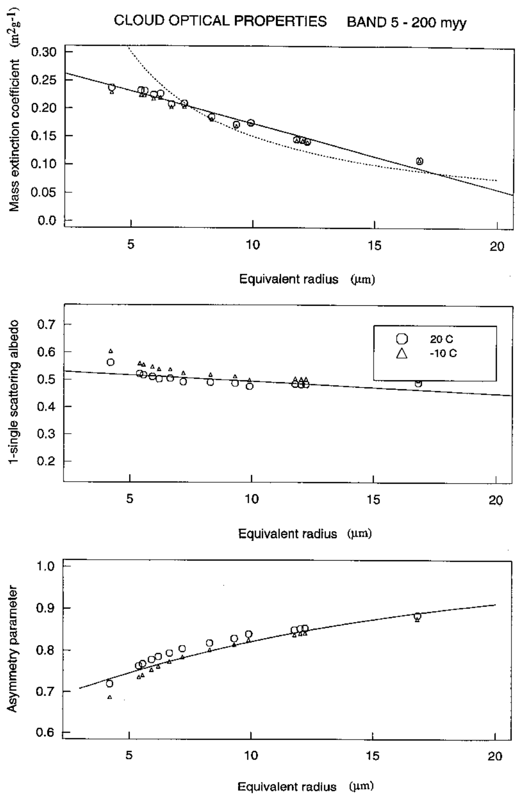


*Fig. 8.* The broadband (5–200 µm) mass extinction coefficient $\beta_{ext}$/LWC (m$^2$g$^{-1}$), 1-$\omega$ and $g$ for 14 clouds as a function of effective radius $r_e$ (µm), for temperatures 20°C and −10°C. Solid lines are parametrizations (14); dotted line is the large-drop approximation (10).

The division of the 8–12.5 µm (b2) region into sub-bands is now less important (unlike for $k_c$), as the present parameters ($\beta_{ext}$, 1-$\omega$, $g$) are associated with $\lambda \approx 12.5$ µm, rather than 10 µm, as the natural turnpoint in their spectral behaviour in Fig. 4. Therefore the three-band parameterization (15) should be useful enough for most wide- and narrowband two-stream LW schemes.

## 5. Application examples

For test purposes, the parameterizations of Section 4 were implemented both to a delta-two-stream LW scheme (Ritter and Geleyn, 1992; in DWD GCM), and to an emissivity scheme. The latter is based on the 6-band LW scheme of

Morcrette (1991; in ECMWF GCM), slightly modified for use in the University of Helsinki mesoscale model. (The modifications include a simplified temperature dependence of gas absorption, which avoids the convergence problem discussed in Räisänen (1996), and the neglect of $O_3$, $CH_4$, $N_2O$ and CFCs; they make the code a lot faster without much penalty in accuracy for the lower troposphere). The McClatchey midlatitude summer atmosphere with 300 ppmv of CO2 was used, and calculations for several cloudy cases with and without precipitation were performed. Results are given in Fig. 9 and in Table 2.

In Fig. 9 results are shown for a nonprecipitating water cloud at 3–4 km altitude. The outgoing longwave radiation, downwelling LW radiation at the surface, and the cloud layer heating rate are shown as a function of cloud liquid water path for the three-band emissivity scheme version (12), using two cloud drop effective radii, 5 and 17 μm. Also shown are the differences due to using the broadband version in the emissivity scheme ((11) versus (12)), and in the delta-two-stream scheme ((14) versus (15)).

First, it can be noted that for a given LWP, the effective radius can have a considerable effect in the long-wave region. For instance, for LWP$=$ 10 $gm^{-2}$, the downward flux at the surface is 16 $Wm^{-2}$ larger for $r_e=5$ μm than for $r_e=17$ μm in the emissivity scheme. A similar 17 $Wm^{-2}$ increase is obtained also in the two-stream scheme (not shown). Therefore, use of a constant mass absorption coefficient does not seem appropriate. Second, the effect of using the broadband version is to systematically increase the downward flux at the surface, to decrease outgoing longwave radiation, and to slightly increase the cloud LW cooling, that is, to make the cloud more opaque. The differences reach 5–7 $Wm^{-2}$ in $F_{down,surface}$ for the small-drop cloud for LWP$=$3–10 $gm^{-2}$ in both schemes. The sensitivity of the results as well to $r_e$ as to the spectral optics is largest for intermediate LWP (i.e. for semi-transparent clouds); for small LWP the cloud has small effect anyway, and for large LWP, the cloud becomes a blackbody.

The rainy case results (Table 2) include two cloud layer altitudes and four precipitation rates. The cloud drop LWC and $r_e$ are fixed to 1 $gm^{-3}$ and 17 μm, respectively, but the results are insensitive to this choice as far as the cloud is optically thick. The effect of precipitation on OLR is negligible. However, the downward flux at the surface is affected more (for cloudbase at 3 km, by about $+5$, $+15$ and $+24$ $Wm^{-2}$ for rain rates of 1, 10 and 100 mm/h). Also the LW cooling of the cloud layer is increased somewhat. This additional cooling is actually not caused by the rain drops within

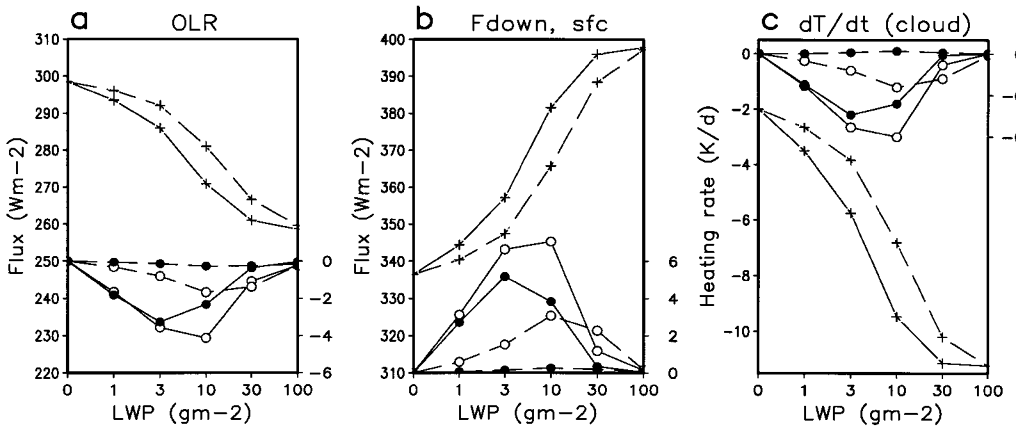


*Fig. 9.* A cloud is located at 3–4 km in the midlatitude summer atmosphere, solid (dashed) curves stand for an effective radius of 5 (17) μm. (a) Outgoing longwave radiation. + stands for the results of the three-band parameterization (12) in the emissivity scheme. Open circles are the difference (expanded scale on the right) between the broadband (11) and the 3-band parameterization (12) in the emissivity scheme, and solid circles the similar difference ((14) versus (15)) in the delta-two-stream scheme. (b) As (a) but for the downwelling longwave flux at the surface. (c) As (a) but for the average heating rate in the cloud layer.

Table 2. *Results for non-precipitating cloud/precipitating cloud (emissivity scheme only)*

| | OLR (W $m^{-2}$) | $F_{down,surface}$ (W $m^{-2}$) | $(dT/dt)_{cloud}$ (K/d) |
|---|---|---|---|
| clear sky column: | 298.49 | 336.49 | |
| cloud at 1–2 km: | | | |
| $R=0$ mm/h | 283.18 | 413.29 | −9.77 |
| $R=1$ mm/h | 0.00 | +0.88 | −0.07 |
| $R=10$ mm/h | 0.00 | +3.61 | −0.29 |
| $R=100$ mm/h | −0.01 | +8.97 | −0.74 |
| cloud at 3–4 km: | | | |
| $R=0$ mm/h | 257.84 | 398.23 | −11.23 |
| $R=1$ mm/h | 0.00 | +4.89 | −0.58 |
| $R=10$ mm/h | 0.00 | +15.05 | −1.87 |
| $R=100$ mm/h | 0.00 | +24.00 | −3.20 |

For the cloud droplets, LWP $=1000$ gm$^{-2}$ and $r_e=17$ μm in all cases. MLS atmosphere and 300 ppmv of $CO_2$ is assumed. In cases with rain rate $R>0$, the *changes* compared to the non-precipitating cloud case ($R=0$) are given.

the cloud, but by those below it, which decrease the upward flux entering the cloudbase. The cooling rates below the cloud are likewise affected, albeit less.

The effect of precipitation is critically dependent on the cloudbase altitude (via the temperature difference between the surface and the cloud base), and is much less when $z_b=1$ km rather than 3 km. Also, the effect is likely to decrease with increasing humidity below cloud. As high cloud bases and dry lower atmosphere conditions seldom co-occur with heavy precipitation, the average effect of rain on LW radiation may be small enough to be neglected in most applications.

## 6. Conclusion

Clear-sky longwave line-by-line calculations and spectral observations display strong wavelength dependence in the atmospheric longwave radiative fluxes. The GCM radiation parameterizations try to mimick that by using several longwave spectral bands; yet the way clouds are handled is very simple in most of them. Typically the same mass absorption coefficient is used for all LW bands and for all water clouds. We have calculated the LW cloud optics for several cloud types and for rain, using Mie theory. We then have parameterized the optics for broadband and for some practical widebands; this was done both for two-stream type and for emissivity-type applications. The input parameters are the cloud effective radius $r_e$, cloud liquid water content LWC, and rain rate $R$. If $r_e$ is not provided by the host model, a simple relation between it and LWC is given, separately for maritime and continental air masses.

In the cloud LW optics, the mass absorption coefficient shows a "droplet window" at 7–10 μm for small-drop clouds; and smaller values for large $r_e$ in general. The extinction coefficient does not show a clear window effect but the coalbedo 1-$\omega$ does. The rain LW optics follow the large absorbing drop approximation closely but the impact is not important inside a precipitating cloud. Parameterizations are given anyway, as some applications (e.g. rainy layers below cloud) might find some use for them.

The suggested cloud and rain parameterizations try to include the salient features of the above $\lambda$- and $r_e$-dependences in a simple and practical fashion. For short-range weather forecast models (e.g., HIRLAM), use of the $r_e$-dependent broadband mass absorption coefficient (11) should be a good compromise between speed and accuracy. For GCMs, the three- or four-band schemes are recommended, as the overlap of the gaseous and the droplet spectra will then be handled more accurately.

## 7. Acknowledgement

The work is part of the Nordic Climate Modelling Project (NOCLIMP).

## REFERENCES


Bohren, C. F. and Huffman, D. R. 1983. *Absorption and scattering of light by small particles.* Wiley & Sons, 530 pp.

Chylek, P. 1978. Extinction and liquid water content of fogs and clouds. *J. Atmos. Sci.*, **35**, 296–300.

Chylek, P. and Ramaswamy, V. 1982. Simple approximation for infrared emissivity of water clouds. *J. Atmos. Sci.*, **39**, 171–177.

Chylek, P., Damiano, P. and Shettle, E. P. 1992. Infrared emittance of waterclouds. *J. Atmos. Sci.* **49**, 1459–1472.

Ebert, E. and Curry, J. 1992. A parameterization of ice cloud optical properties for climate models. *J. Geophys. Res.* **97** D4, 3831–3836.

Fouquart, Y. 1988. Radiative transfer in climate models. In: *Physically-based modelling and simulation of climate and climatic change.* NATO ASI Series C, **243**, Kluwer, 223–284.

Francis, P. N., Jones, A., Saunders, R. W., Shine, K. P., Slingo, A. and Sun, Z. 1994. An observational and theoretical study of the radiative properties of cirrus: some results from ICE'89. *Quart. J. Roy. Meteor. Soc.* **120**, 809–848.

Hale, G. M. and Querry, M. R. 1973. Optical constants of water in the 200 nm to 200 μm wavelength region. *Appl. Optics* **12**, 555–563.

Hu, Y. X. and Stamnes, K. 1993. An accurate parameterization of the radiative properties of water clouds suitable for use in climate models. *J. Clim.* **6**, 728–742.

Johnson, D. W. 1993. Parameterisation of the cloud topped boundary layer: Aircraft measurements. In ECMWF Workshop Proceedings: *Parameterization of the cloud topped boundary layer*, ECMWF, Reading, UK, 77–117.

Liou, K. N. 1992. *Radiation and cloud processes in the atmosphere.* Oxford University Press, 487 pp.

Martin, G. M., Johnson, D. W. and Spice, A. 1994. The measurement and parameterization of effective radius of droplets in warm stratocumulus cloud. *J. Atmos. Sci.* **51**, 1823–1842.

Nicholls, S. 1984. The dynamics of stratocumulus: aircraft observations and comparisons with a mixed layer model. *Quart. J. Roy. Meteor. Soc.* **110**, 783–820.

Pinnick, R. G., Jennings, S. G., Chylek, P. and Auvermann, H. J. 1979. Verification of a linear relation between IR extinction, absorption and liquid water content of fogs. *J. Atmos. Sci.* **36**, 1577–1586.

Pontikis, C. and Hicks, E. 1992. Contribution to the cloud droplet effective radius parameterisation. *Geophys. Res. Letters* **19**, 2227–2230.

Roeckner, E., Arpe, K., Bengtsson, L., Christoph, M., Claussen, M., Dumenil, L., Esch, M., Giorgetta, M., Schlese, U. and Schulzweida, U. 1996. The atmospheric general circulation model ECHAM-4: Model description and simulation of present-day climate. Report 218, Max-Planck Institute for Meteorology, Hamburg, Germany, 90 pp.

Räisänen, P. 1996. The effect of vertical resolution on clear-sky radiation calculations: tests with two schemes. *Tellus* **48A**, 403–423.

Savijärvi, H., Arola, A. and Räisänen, P. 1997. Short-wave optical properties of precipitating water clouds. *Quart. J. Roy. Meteor.Soc.* **123**, 883–899.

Savijärvi, H. 1997. Short-wave optical properties of rain. *Tellus*, **49A**, 177–181.

Slingo, A. and Schrecker, H. 1982. On the shortwave radiative properties of stratiform water clouds. *Quart. J. Roy. Meteor. Soc.* **108**, 407–426.

Stephens, G. L. 1978. Radiation profiles in extended water clouds II: Parameterization schemes. *J. Atmos. Sci.* **35**, 2123–2132.

Stephens, G. L., Paltridge G. W. and Platt, C. M. R. 1978. Radiation profiles in extended water clouds III: Observations. *J. Atmos. Sci.* 35, 2133–2141.

Stephens, G. L. 1979. *Optical properties of eight water cloud types.* CSIRO Atmos.Phys.Tech.Pap., **36**, Melbourne, Australia. 36pp.

Stephens, G. L. 1984. The parameterization of radiation for numerical weather prediction and climate models. *Mon. Wea. Rev.* **112**, 826–867.